

Cosmological Parameter Estimation with a Joint-Likelihood Analysis of the Cosmic Microwave Background and Big Bang Nucleosynthesis

Cara Giovanetti,^{1,*} Mariangela Lisanti,^{2,3,†} Hongwan Liu,^{4,5,6,‡}
Siddharth Mishra-Sharma,^{7,8,9,§} and Joshua T. Ruderman^{1,¶}

¹*Center for Cosmology and Particle Physics, Department of Physics,
New York University, New York, NY 10003, USA*

²*Department of Physics, Princeton University, Princeton, NJ 08544, USA*

³*Center for Computational Astrophysics, Flatiron Institute, 162 Fifth Ave, New York, NY 10010, USA*

⁴*Physics Department, Boston University, Boston, MA 02215, USA*

⁵*Kavli Institute for Cosmological Physics, University of Chicago, Chicago, IL 60637*

⁶*Theoretical Physics Department, Fermi National Accelerator Laboratory, Batavia, IL 60510*

⁷*The NSF AI Institute for Artificial Intelligence and Fundamental Interactions*

⁸*Center for Theoretical Physics, Massachusetts Institute of Technology, Cambridge, MA 02139, USA*

⁹*Department of Physics, Harvard University, Cambridge, MA 02138, USA*

(Dated: August 28, 2024)

We present the first joint-likelihood analysis of Big Bang Nucleosynthesis (BBN) and Cosmic Microwave Background (CMB) data. Bayesian inference is performed on the baryon abundance and the effective number of neutrino species, N_{eff} , using a CMB Boltzmann solver in combination with LINX, a new flexible and efficient BBN code. We marginalize over Planck nuisance parameters and nuclear rates to find $N_{\text{eff}} = 3.08^{+0.13}_{-0.13}$, $2.94^{+0.16}_{-0.16}$, or $2.98^{+0.14}_{-0.13}$, for three separate reaction networks. This framework enables robust testing of the Lambda Cold Dark Matter paradigm and its variants with CMB and BBN data.

Introduction.—Both the Cosmic Microwave Background (CMB) and the primordial abundance of light elements produced during Big Bang Nucleosynthesis (BBN) provide a wealth of information about the early Universe and its constituents. Precision measurements of the CMB have tightly constrained the Lambda Cold Dark Matter (Λ CDM) cosmological parameters, with corroborating measurements from BBN painting a largely consistent picture of the Universe at early times.

The CMB power spectrum is at the forefront of precision cosmology, providing percent-level measurements of the Λ CDM cosmological parameters (*e.g.* the baryon abundance, $\Omega_b h^2$) and constraining alternative scenarios (*e.g.* changes to the effective number of neutrino species, N_{eff}). Analyses performed on Planck data [1] often employ Bayesian inference using sampling methods like Markov-Chain Monte Carlo (MCMC) or nested sampling to explore the high-dimensional parameter space, including a large number of nuisance parameters. Such detail is now expected even in studies exploring new-physics signatures, such as Refs. [2, 3].

Meanwhile, BBN provides a unique window into the epoch when the baryon temperature was in the keV–MeV range. The baryon density can impact primordial element abundances, since a higher density allows newly-formed nuclei to interact more frequently, fusing

them into heavier elements. Recent experimental determinations of D/H (the number density ratio of deuterium to hydrogen nuclei) [4–7] and Y_{P} (the mass abundance of helium-4) [8–14] have reached percent-level precision. This, combined with theoretical predictions for the abundance of these nuclides using public BBN codes [15–19], allows for a percent-level determination of $\Omega_b h^2$, rivaling that of the CMB. Uncertainties in the theoretical predictions are dominated by the uncertainty in the rates of nuclear reactions (including the neutron lifetime) occurring during BBN; these have been studied carefully for many different reactions in *e.g.* Refs. [20–27]. In practice, each rate’s uncertainty is modeled by a nuisance parameter; accurate Y_{P} and D/H predictions require marginalizing over parameters for all reactions that significantly influence these abundances. BBN can also provide an independent constraint on N_{eff} , since a larger N_{eff} increases the expansion rate, increasing Y_{P} by reducing the time available for weak interactions to convert neutrons to protons, and increasing D/H by ending deuterium burning earlier.

Despite the importance of BBN to the Λ CDM and Λ CDM+ N_{eff} models, a joint fit accounting for all CMB and BBN nuisance parameters has so far not been performed. Publicly-available BBN codes either have relatively long runtimes or are structured such that nuclear rate uncertainties cannot be easily varied over, making them difficult to combine with standard parameter estimation frameworks such as MCMC samplers. Instead, previous analyses have focused on performing either the BBN or the CMB side of the analysis relatively well, while including information from the other in a less rigorous manner. For example, the Planck Collaboration performed a joint CMB power spectrum and BBN anal-

* cg3566@nyu.edu; ORCID: 0000-0003-1611-3379

† mlisanti@princeton.edu; ORCID: 0000-0002-8495-8659

‡ hongwan@bu.edu; ORCID: 0000-0003-2486-0681

§ smsharma@mit.edu; ORCID: 0000-0001-9088-7845; Currently at Anthropic; work performed while at MIT/IAIFI.

¶ ruderman@nyu.edu; ORCID: 0000-0001-6051-9216

ysis, marginalizing over all Planck experimental nuisance parameters, but using either a constant theory uncertainty on the D/H and Y_P predictions [1] or marginalizing over just one reaction rate [28], in an attempt to encapsulate the effects of all the nuclear rate uncertainties. On the other hand, BBN-focused analyses (*e.g.* Refs. [16, 26, 29, 30]) usually vary the nuclear rates to better capture the uncertainty in the predicted abundance, but frequently use only a CMB prior on $\Omega_b h^2$. Neither case can account for correlated uncertainties between cosmological parameters, CMB experimental nuisance parameters, and BBN nuisance parameters.

Furthermore, the CMB power spectrum is dependent on Y_P through its impact on the damping tail. Therefore, correctly predicting the power spectrum for given values of $\Omega_b h^2$ and N_{eff} requires the BBN prediction of Y_P at these parameter values. This is not accounted for in BBN-focused analyses. For CMB-focused analyses, Boltzmann codes such as CLASS [31–34] or CAMB [35, 36] rely on a table of predicted Y_P as a function of $\Omega_b h^2$ and N_{eff} . This does not properly capture the uncertainty in the BBN prediction, and also must be recomputed for other alternatives to Λ CDM.

Ref. [37] (hereinafter [Paper I](#)) introduces the new public BBN code LINX (Light Isotope Nucleosynthesis with JAX) and its underlying computational formalism. LINX is written with JAX [38, 39]—a Python-based framework that allows for fast compiled code—and is structured for efficient parameter estimation using MCMC samplers. This *Letter* uses BBN abundance predictions from LINX to perform Bayesian inference on cosmological parameters. We perform a BBN-only inference of $\Omega_b h^2$ (with N_{eff} fixed) and $\Omega_b h^2 + N_{\text{eff}}$, marginalizing over the nuclear rate uncertainties. We then generalize these to CMB+BBN analyses, using the Boltzmann code CLASS [31–34] for the CMB power spectrum prediction. The joint Bayesian analysis—the first of its kind—varies all cosmological parameters, Planck nuisance parameters, and BBN nuisance parameters, while including the BBN prediction of Y_P in the CMB power spectrum prediction.

BBN-only Analysis.— To begin, we perform a BBN-only study to infer $\Omega_b h^2$ (with N_{eff} fixed) and $\Omega_b h^2 + N_{\text{eff}}$ using LINX. In the latter, we add an inert, relativistic species that can have a positive or negative energy density (negative energy density being an unphysical scenario that can, however, mimic colder-than-expected neutrinos), following *e.g.* Refs. [1, 30]. The rate for each nuclear reaction i is $r_i(T) \equiv u^{-1} \langle \sigma v \rangle(T)$, where u is the atomic mass unit, $\langle \sigma v \rangle$ is the velocity-averaged cross section, and T is the baryon temperature—see *e.g.* Ref. [16] for discussion of the unit convention. This *Letter* adopts three separate sets of reaction rates: 1) “PRIMAT”, the default small network used by the PRIMAT BBN code [16], 2) “PARthENoPE”, a set of rates extracted from the PARthENoPE BBN code [26], and 3) “YOF”, a set of rates used by Ref. [40], provided by the PRyMordial BBN code [19]. Following Refs. [16, 41], the rate uncertainties are captured by taking r_i to be log-normally

distributed, with a mean value $\bar{r}_i(T)$ and standard deviation $\sigma_i(T)$. Specifically, $\log r_i(T) = \log \bar{r}_i(T) + q_i \sigma_i(T)$, where q_i is a unit Gaussian random variable. The BBN nuisance parameters, denoted as ν_{BBN} , are q_i and the neutron lifetime.

To obtain $\bar{r}_i(T)$ and $\sigma_i(T)$, measurements of the cross section as a function of energy are combined across different experiments, and a fit to the data is performed before velocity-averaging. Each set of rates makes different choices on the fitting procedure and the experimental data that are used. PARthENoPE performs purely phenomenological polynomial fits to the data [26]. PRIMAT fits the data using functional forms derived from *ab initio* theory calculations [20, 27]. YOF relies mainly on results provided by the NACREII Collaboration, which uses experimental data to fit a potential model for each nuclear reaction [42]. All three sets incorporate the recent measurement of the $d(p, \gamma)^3\text{He}$ rate from 30 keV–300 keV by the LUNA Collaboration [25].

Because of the different approaches taken, these sets of rates also make different predictions. D/H predictions based on PRIMAT are in 1.8σ tension with the observed abundance, whereas predictions based on PARthENoPE and YOF are not [26, 27]. Experimental determinations of $d(d, n)^3\text{He}$ and $d(d, p)t$ will be crucial for reducing the uncertainty in the prediction of D/H, and may resolve these discrepancies [26, 27, 43].

We construct a BBN likelihood using the observed D/H determined by Ref. [6] and Y_P from Ref. [8]:

$$\begin{aligned} \text{D/H}^{\text{obs}} &= 2.527 \times 10^{-5} & \sigma_{\text{D/H}^{\text{obs}}} &= 0.030 \times 10^{-5} \\ Y_P^{\text{obs}} &= 0.2449 & \sigma_{Y_P^{\text{obs}}} &= 0.004. \end{aligned}$$

The BBN log-likelihood is given by

$$\begin{aligned} -2 \log \mathcal{L}_{\text{BBN}} &= \left(\frac{Y_P^{\text{pred}}(\Omega_b h^2, N_{\text{eff}}, \nu_{\text{BBN}}) - Y_P^{\text{obs}}}{\sigma_{Y_P^{\text{obs}}}} \right)^2 \\ &+ \left(\frac{\text{D/H}^{\text{pred}}(\Omega_b h^2, N_{\text{eff}}, \nu_{\text{BBN}}) - \text{D/H}^{\text{obs}}}{\sigma_{\text{D/H}^{\text{obs}}}} \right)^2, \quad (1) \end{aligned}$$

where LINX computes $Y_P^{\text{pred}}(\Omega_b h^2, N_{\text{eff}}, \nu_{\text{BBN}})$ and $\text{D/H}^{\text{pred}}(\Omega_b h^2, N_{\text{eff}}, \nu_{\text{BBN}})$.

We use dynesty [44, 45] to perform nested sampling [46, 47], specifying bounding and static sampling methods as in Refs. [48–51]. Nested sampling for parameter inference has a number of advantages over methods like MCMC, chief among them adaptability for complex, multimodal posteriors and ease of computing Bayesian evidence (see *e.g.* [52]). This facilitates marginalization over the nuisance parameters in our analyses. Details of the computational analysis are discussed in Appendix A.

We include 12 key nuclear reactions to determine $Y_P^{\text{pred}}(\Omega_b h^2, N_{\text{eff}}, \nu_{\text{BBN}})$ and $\text{D/H}^{\text{pred}}(\Omega_b h^2, N_{\text{eff}}, \nu_{\text{BBN}})$; including additional reactions results in changes to the predictions that are well within experimental uncertainties (see [Paper I](#)). Including the neutron lifetime and

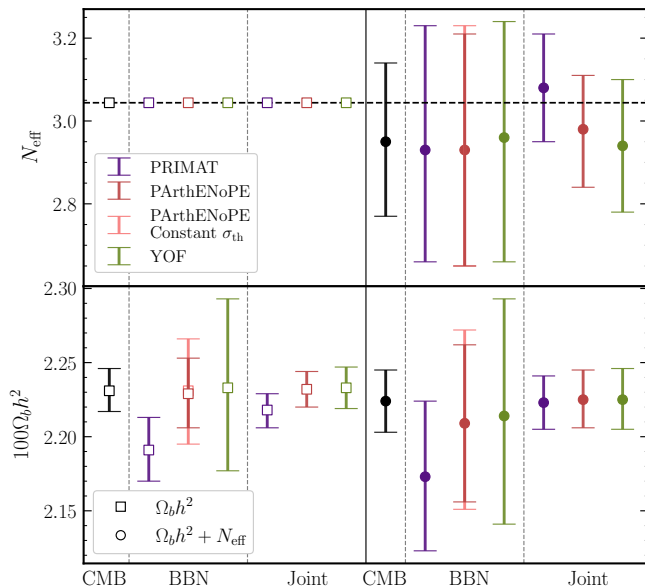


FIG. 1. Parameter medians and 68% credible limits with the inclusion of Planck data only, BBN data only, and both BBN and Planck data, as labeled at the bottom of the figure. Values from individual analyses line up top-to-bottom. Square markers in the left set of columns indicate N_{eff} is held fixed, while circular markers in the right set of columns indicate analyses where N_{eff} is allowed to float. The Λ CDM value of $N_{\text{eff}} = 3.045$ is indicated with the black dashed line. Purple, red, and green points use the PRIMAT, PARthENoPE, and YOF networks, respectively. Pink points indicate that a constant uncertainty is added to the deuterium part of the BBN likelihood. Otherwise, all available nuisance parameters are marginalized over.

the cosmological parameters $\Omega_b h^2$ (and N_{eff}), there are 14 (15) parameters in total. We choose flat priors for cosmological parameters, a Gaussian prior of 879.4 ± 0.6 s [53] for the neutron lifetime, and a unit Gaussian prior for all 12 q_i 's.

Fig. 1 summarizes the main results of this *Letter*; numerical values for these and other analyses are compiled in Appendix B for reference. To validate LINX, we compare the results in the “BBN only” column with those reported in Ref. [54]; for the PRIMAT and YOF networks, there is excellent agreement for both $\Omega_b h^2$ and $\Omega_b h^2 + N_{\text{eff}}$.

When using the PRIMAT and YOF networks, Ref. [54] marginalizes over the nuclear rate uncertainties. However, because of the structure of the PARthENoPE code, Ref. [54], along with Refs. [1, 26], uses a constant theory uncertainty σ_{th} on D/H^{pred} to estimate the nuclear rate uncertainties on the PARthENoPE rates. Here, to mimic this simplified procedure, the theory uncertainty σ_{th} is computed by sampling the relevant rates at a particular parameter combination that is expected to be near the mean of the posterior [1, 26, 54]. However, the uncertainty in the D/H prediction is not constant with respect to $\Omega_b h^2$ and N_{eff} , as shown in Appendix C. Improving

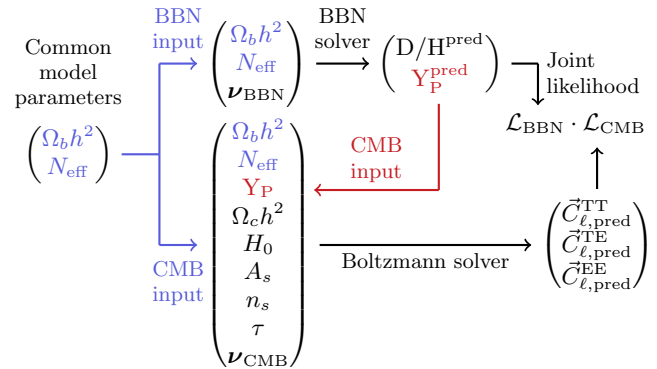


FIG. 2. A schematic illustrating the joint likelihood used for the CMB+BBN analyses. Note that each likelihood is computed at the same values of the input parameters $\Omega_b h^2$ and N_{eff} , and the $Y_{\text{P}}^{\text{pred}}$ output of the BBN solver is used as input to the Boltzmann solver to ensure consistency.

on this situation, LINX allows one to perform the fully marginalized BBN-only analysis with the PARthENoPE rates (solid red lines in Fig. 1). The corresponding LINX result for constant σ_{th} is shown in pink, and is in good agreement with the PARthENoPE results in Ref. [54]. For both $\Omega_b h^2$ and $\Omega_b h^2 + N_{\text{eff}}$, proper marginalization of the nuclear rates increases the precision on $\Omega_b h^2$ by ~ 15 –30%.

Joint CMB+BBN Analyses.— LINX can also be used in conjunction with a CMB Boltzmann code to provide a joint inference of cosmological parameters. We use the Boltzmann code CLASS and include one massive neutrino with mass $m_\nu = 0.06$ eV, consistent with analyses in Ref. [1].

A schematic of the joint likelihood used for a Bayesian inference of $\Omega_b h^2 + N_{\text{eff}}$ is included in Fig. 2. Given $\Omega_b h^2$, N_{eff} , and BBN nuisance parameters, LINX computes D/H^{pred} and $Y_{\text{P}}^{\text{pred}}$ to evaluate \mathcal{L}_{BBN} in Eq. (1). The same $\Omega_b h^2$, N_{eff} , and $Y_{\text{P}}^{\text{pred}}$ —with the other Λ CDM and Planck nuisance parameters—are passed to CLASS and the Planck likelihood to predict power spectra and obtain \mathcal{L}_{CMB} . The joint likelihood is then used for Bayesian inference. Importantly, $Y_{\text{P}}^{\text{pred}}$ needs to be passed to CLASS from a BBN solver, since it has a significant impact on the predicted power spectrum.

Throughout, we use the `Plik` TT+TE+EE likelihood [55], which contains high- ℓ multipoles, and the `commander` lowT and `simall` lowE likelihoods at low- ℓ , for the CMB likelihood. In our joint analyses, we sample 40–41 parameters in the joint analysis, depending on whether N_{eff} is fixed and use `Plik`-recommended priors for the CMB nuisance parameters (or priors from Ref. [56] if unavailable). Broad, flat priors are used for the other CMB model parameters. Our inferred $100\Omega_b h^2$ and $\Omega_b h^2 + N_{\text{eff}}$ with only Planck data are included in Fig. 1 in the “CMB-only” column for reference and are in excellent agreement with Ref. [1].

The joint analysis results are shown under the

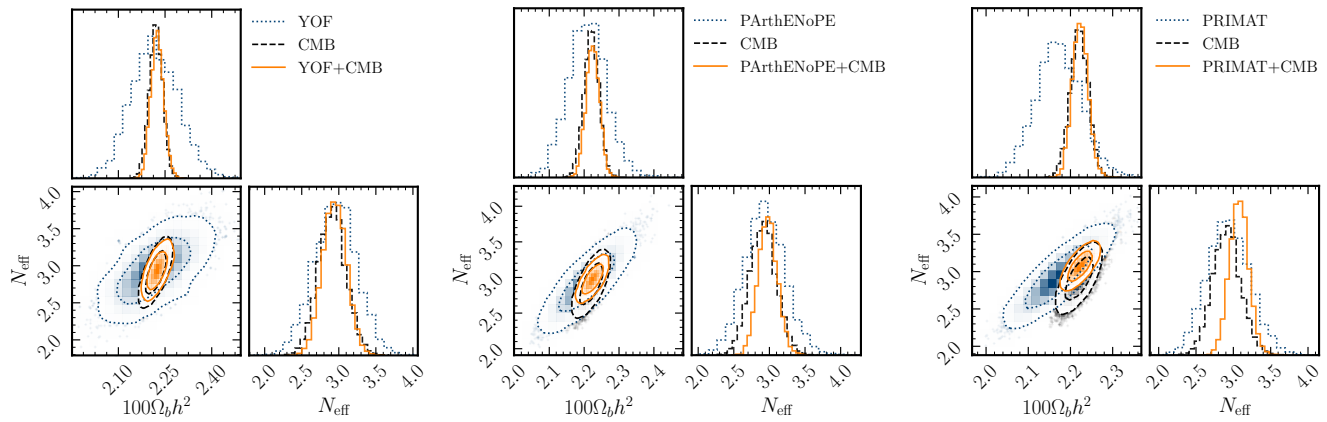


FIG. 3. 68% and 95% contours in the $\Omega_b h^2 - N_{\text{eff}}$ plane for YOF (left), PArthENoPE (center), and PRIMAT (right) nuclear reaction networks. In each panel, the light-blue dotted contours correspond to the BBN-only analysis, the black-dashed to the CMB-only analysis, and the orange-solid to the joint CMB+BBN analysis. All CMB and BBN nuisance parameters are marginalized over. When using the PRIMAT network, the resulting value of N_{eff} in the joint analysis is pushed high. When using the YOF network, the constraining power of BBN is minimal.

“CMB+BBN” column in Fig. 1. The square markers show the inferred $100\Omega_b h^2$, holding N_{eff} fixed. For all three reaction networks, there is a shift in the medians and error bars towards the CMB-preferred value of $100\Omega_b h^2 = 2.231^{+0.015}_{-0.014}$. Compared to the BBN-only results, the error bars are reduced in the joint results; this is most pronounced for the joint constraint with the YOF network, where the error bars shrink by a factor of ~ 3 . The PRIMAT joint result ($2.218^{+0.012}_{-0.011}$) is most discrepant with the CMB-only result, due to the low BBN-only preferred value for $100\Omega_b h^2$ ($2.191^{+0.022}_{-0.021}$).

A simplified version of this analysis is performed in Ref. [16] using the PRIMAT network. For that study, the Planck posterior [1] for $\Omega_b h^2$ is used as a prior in the BBN-only likelihood, so only the BBN likelihood must be computed for each sample. When using LINX to perform this simplified analysis using the Planck 2018 result of $100\Omega_b h^2 = 2.236^{+0.015}_{-0.015}$ [1] as the prior, we find that $100\Omega_b h^2 = 2.215^{+0.011}_{-0.011}$, which is slightly lower than the results with a full CMB analysis.

Next, we vary N_{eff} in addition to the six Λ CDM parameters, the BBN rate uncertainties, and the CMB nuisance parameters. For the PArthENoPE and YOF rates, including a BBN likelihood in this analysis does not dramatically shift many of the cosmological parameters away from their inferred values in a CMB-only analysis. This is because of the good agreement between the PArthENoPE network’s predictions and measurements, as well as YOF’s wide error bars on the reactions in its network, which decreases its constraining power. These effects are illustrated in the first two panels of Fig. 3, where the individual posteriors overlap with each other. These results are also included in Fig. 1 in the “CMB+BBN” column for comparison.

However, the individual posteriors for the PRIMAT network, shown in the third panel of Fig. 3, are in slight

discrepancy with each other, which influences the inferred values of $\Omega_b h^2$ and N_{eff} . The inferred value for N_{eff} increases to $3.08^{+0.13}_{-0.13}$, from the CMB-only prediction of $2.95^{+0.19}_{-0.18}$ and the BBN-only prediction of $2.93^{+0.30}_{-0.27}$. The correlation between N_{eff} and $\Omega_b h^2$, and the resulting adjustment of the inferred values away from those attained in a CMB-only analysis, are responsible for the higher inferred value of N_{eff} .

Ref. [1] observed a similar effect on the best-fit parameters when using the PRIMAT rates and a constant theory uncertainty σ_{th} on D/H and Y_{p} . However, a fully marginalized analysis with LINX allows one to uncover correlations between nuisance parameters, including how nuclear rates have to adjust to accommodate the preferred region for the CMB+BBN fit. Fig. 4 shows the marginalized posterior for three deuterium burning reactions ($d(p, \gamma)^3\text{He}$, $d(d, n)^3\text{He}$, and $d(d, p)t$) for the $\Omega_b h^2$ analysis. Decreased rates for all three reactions are required to bring BBN into better agreement with Planck data using PRIMAT.

The joint analyses discussed above also have implications for the Λ CDM+ N_{eff} parameters that do not have direct impacts on BBN. When N_{eff} is allowed to float, including BBN in a joint analysis leads to smaller error bars in N_{eff} , which can propagate to noticeably smaller error bars in these parameters. For instance, when N_{eff} floats, the joint analysis gives error bars on the Hubble parameter and dark matter density that are $\sim 30\%$ smaller than the error bars on their CMB-only determinations.

Conclusions.— This study reveals the importance of proper accounting of the CMB and BBN nuisance parameters in a joint CMB+BBN analysis, as well as including the impacts of BBN on the determination of $\Omega_b h^2$ and Y_{p} . Consistent analyses like those described in this *Letter* are essential for testing cosmological mod-

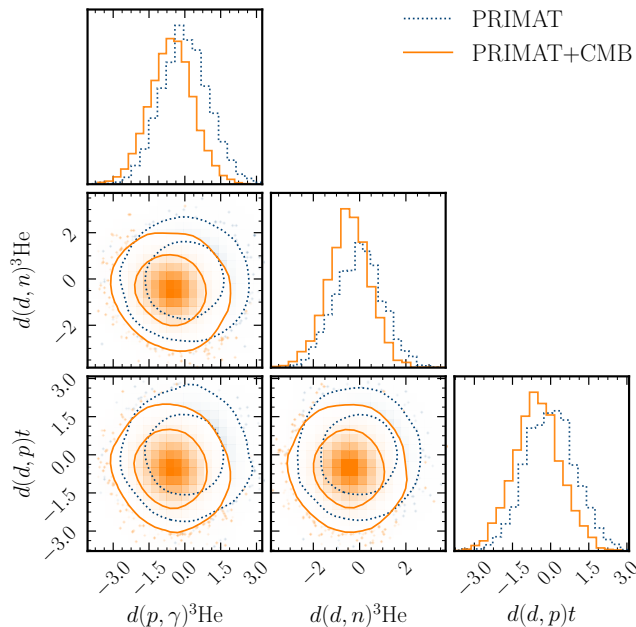


FIG. 4. 68% and 95% posterior contours for the nuisance parameters q_i that determine the scaling of three key deuterium burning rates in the PRIMAT network. The BBN-only analysis (blue, dashed) is compared to a joint CMB+BBN analysis (orange, solid), allowing $\Omega_b h^2$ to float and fixing $N_{\text{eff}} = 3.045$. In the joint analysis, these rates are pushed away from their central values to attain a better joint fit with the CMB.

els. The CMB+BBN results come at little computational cost; LINX is fast enough that the time taken to evaluate the joint likelihood is dominated by the Boltzmann solver. We include a complete index of the standard cosmological results in Appendix B. Our analyses also explore systematic effects from choosing different reaction networks—depending on which network is used, BBN can have little constraining power, can validate CMB analyses, or can pull parameters away from their CMB-only values.

Moving forward, LINX can be used in conjunction with cosmology sampling frameworks such as *cosmomc* [57], *MontePython* [58], and other tools for cosmology data analysis. Additionally, LINX greatly facilitates the extension of joint CMB+BBN fits to new-physics scenarios, including electromagnetically coupled WIMPs [59–62], neutrino-coupled WIMPs [63, 64], MeV-scale axion-like particles [65], and hidden sector particles such as millicharged particles with dark radiation [66]. LINX can also be used to obtain an improved joint BBN+BAO determination of the Hubble constant, a crucial piece of the Hubble tension puzzle [67].

ACKNOWLEDGEMENTS

We thank the PRyMordial team (Anne-Katherine Burns, Tim Tait, and Mauro Valli) for early access to their code and assistance with setup and usage throughout the beta-testing phase. We thank Nick dePorzio, Colin Hill, and Zilu Zhou for help with CLASS. We further thank Zilu Zhou for help with the *Plik* likelihoods. We thank Mark Paris for information about the measurement of deuterium reaction rates. We thank the JAX team and the individuals who assisted us with JAX and JAX packages, including Dan Foreman-Mackey, Peter Hawkins, and Patrick Kidger. We thank Julien Lesgourgues and Nils Schöneberg for comments on a draft of this paper. ML is supported by the Department of Energy (DOE) under Award Number DE-SC0007968 as well as the Simons Investigator in Physics Award. HL was supported by the Kavli Institute for Cosmological Physics and the University of Chicago through an endowment from the Kavli Foundation and its founder Fred Kavli, and Fermilab operated by the Fermi Research Alliance, LLC under contract DE-AC02-07CH11359 with the U.S. Department of Energy, Office of Science, Office of High-Energy Physics. SM is partly supported by the U.S. Department of Energy, Office of Science, Office of High Energy Physics of U.S. Department of Energy under grant Contract Number DE-SC0012567. JTR is supported by NSF grant PHY-2210498. This material is based upon work supported by the NSF Graduate Research Fellowship under Grant No. DGE1839302. This work is supported by the National Science Foundation under Cooperative Agreement PHY-2019786 (The NSF AI Institute for Artificial Intelligence and Fundamental Interactions, <http://iaifi.org/>). This research was supported in part by Perimeter Institute for Theoretical Physics. Research at Perimeter Institute is supported by the Government of Canada through the Department of Innovation, Science and Economic Development and by the Province of Ontario through the Ministry of Research, Innovation and Science. This work was performed in part at the Aspen Center for Physics, which is supported by NSF grants PHY-1607611 and PHY-2210452. This research was supported in part by grant NSF PHY-2309135 to the Kavli Institute for Theoretical Physics (KITP). The work presented in this paper was performed on computational resources managed and supported by Princeton Research Computing. This work was supported in part through the NYU IT High Performance Computing resources, services, and staff expertise. This work makes use of the corner [68], *diffraction* [69], *dynesty* [44, 45], *equinox* [70], *JAX* [38, 39], *matplotlib* [71], *numpy* [72], *schwimmbad* [73], and *scipy* [74] Python packages.

[1] N. Aghanim *et al.*, “Planck2018 results: VI. Cosmological parameters,” *Astronomy & Astrophysics* **641**, A6 (2020).

[2] S. Alvi, T. Brinckmann, M. Gerbino, M. Lattanzi, and L. Pagano, “Do you smell something decaying? Updated

- linear constraints on decaying dark matter scenarios,” *JCAP* **11**, 015 (2022), [arXiv:2205.05636 \[astro-ph.CO\]](#).
- [3] Saurabh Bansal, Jeong Han Kim, Christopher Kolda, Matthew Low, and Yuhsin Tsai, “Mirror twin Higgs cosmology: constraints and a possible resolution to the H_0 and S_8 tensions,” *JHEP* **05**, 050 (2022), [arXiv:2110.04317 \[hep-ph\]](#).
- [4] Ryan J. Cooke, Max Pettini, Kenneth M. Nollett, and Regina Jorgenson, “The primordial deuterium abundance of the most metal-poor damped Ly α system,” *The Astrophysical Journal* **830**, 148 (2016).
- [5] S. Riemer-Sørensen, S. Kotuš, J. K. Webb, K. Ali, V. Dumont, M. T. Murphy, and R. F. Carswell, “A precise deuterium abundance: remeasurement of the $z = 3.572$ absorption system towards the quasar PKS1937–101,” *Monthly Notices of the Royal Astronomical Society* **468**, 3239–3250 (2017).
- [6] Ryan J. Cooke, Max Pettini, and Charles C. Steidel, “One percent determination of the primordial deuterium abundance,” *The Astrophysical Journal* **855**, 102 (2018).
- [7] E O Zavarygin, J K Webb, V Dumont, and S Riemer-Sørensen, “The primordial deuterium abundance at $z = 2.504$ from a high signal-to-noise spectrum of Q1009+2956,” *Monthly Notices of the Royal Astronomical Society* **477**, 5536–5553 (2018).
- [8] Erik Aver, Keith A. Olive, and Evan D. Skillman, “The effects of He I $\lambda 10830$ on helium abundance determinations,” *Journal of Cosmology and Astroparticle Physics* **2015**, 011–011 (2015).
- [9] Erik Aver, Danielle A. Berg, Keith A. Olive, Richard W. Pogge, John J. Salzer, and Evan D. Skillman, “Improving helium abundance determinations with Leo P as a case study,” *Journal of Cosmology and Astroparticle Physics* **2021**, 027 (2021).
- [10] Mabel Valerdi, Antonio Peimbert, Manuel Peimbert, and Andrés Sixtos, “Determination of the primordial helium abundance based on NGC 346, an HII region of the Small Magellanic Cloud,” *The Astrophysical Journal* **876**, 98 (2019).
- [11] Vital Fernández, Elena Terlevich, Angeles I Díaz, and Roberto Terlevich, “A Bayesian direct method implementation to fit emission line spectra: application to the primordial He abundance determination,” *Monthly Notices of the Royal Astronomical Society* **487**, 3221–3238 (2019).
- [12] O A Kurichin, P A Kislitsyn, V V Klimenko, S A Balashev, and A V Ivanchik, “A new determination of the primordial helium abundance using the analyses of hii region spectra from SDSS,” *Monthly Notices of the Royal Astronomical Society* **502**, 3045–3056 (2021).
- [13] Tiffany Hsyu, Ryan J. Cooke, J. Xavier Prochaska, and Michael Bolte, “The PHLEK survey: A new determination of the primordial helium abundance,” *The Astrophysical Journal* **896**, 77 (2020).
- [14] Mabel Valerdi, Antonio Peimbert, and Manuel Peimbert, “Chemical abundances in seven metal-poor HII regions and a determination of the primordial helium abundance,” *Monthly Notices of the Royal Astronomical Society* **505**, 3624–3634 (2021).
- [15] A. Arbey, “AlterBBN: A program for calculating the BBN abundances of the elements in alternative cosmologies,” *Computer Physics Communications* **183**, 1822–1831 (2012).
- [16] Cyril Pitrou, Alain Coc, Jean-Philippe Uzan, and Elisabeth Vangioni, “Precision big bang nucleosynthesis with improved helium-4 predictions,” Submitted to *Phys. Rept.* (2018), [arXiv:1801.08023](#).
- [17] R. Consiglio, P.F. de Salas, G. Mangano, G. Miele, S. Pastor, and O. Pisanti, “PARthENoPE reloaded,” *Computer Physics Communications* **233**, 237–242 (2018).
- [18] A. Arbey, J. Auffinger, K. P. Hickerson, and E. S. Jentsen, “AlterBBN v2: A public code for calculating Big-Bang nucleosynthesis constraints in alternative cosmologies,” (2019), [arXiv:1806.11095 \[astro-ph.CO\]](#).
- [19] Anne-Katherine Burns, Tim M. P. Tait, and Mauro Valli, “PRyMordial: the first three minutes, within and beyond the Standard Model,” *Eur. Phys. J. C* **84**, 86 (2024), [arXiv:2307.07061 \[hep-ph\]](#).
- [20] Á. Gómez Iñesta, C. Iliadis, and A. Coc, “Bayesian estimation of thermonuclear reaction rates for deuterium+deuterium reactions,” *The Astrophysical Journal* **849**, 134 (2017).
- [21] Rafael S. de Souza, S. Reece Boston, Alain Coc, and Christian Iliadis, “Thermonuclear fusion rates for tritium + deuterium using Bayesian methods,” *Phys. Rev. C* **99**, 014619 (2019).
- [22] Rafael S. de Souza, Christian Iliadis, and Alain Coc, “Astrophysical S -factors, thermonuclear rates, and electron screening potential for the ${}^3\text{He}(d,p){}^4\text{He}$ Big Bang reaction via a hierarchical Bayesian model,” *The Astrophysical Journal* **872**, 75 (2019).
- [23] N. Rijal, I. Wiedenhöver, J. C. Blackmon, M. Anastasiou, L. T. Baby, D. D. Caussyn, P. Höflich, K. W. Kemper, E. Koshchiy, and G. V. Rogachev, “Measurement of $d+{}^7\text{Be}$ cross sections for big-bang nucleosynthesis,” *Phys. Rev. Lett.* **122**, 182701 (2019).
- [24] Rafael S. de Souza, Tan Hong Kiat, Alain Coc, and Christian Iliadis, “Hierarchical Bayesian thermonuclear rate for the ${}^7\text{Be}(n,p){}^7\text{Li}$ Big Bang nucleosynthesis reaction,” *The Astrophysical Journal* **894**, 134 (2020).
- [25] V. Mossa *et al.*, “The baryon density of the Universe from an improved rate of deuterium burning,” *Nature* **587**, 210–213 (2020).
- [26] O. Pisanti, G. Mangano, G. Miele, and P. Mazzella, “Primordial deuterium after LUNA: concordances and error budget,” *Journal of Cosmology and Astroparticle Physics* **2021**, 020 (2021).
- [27] Joseph Moscoso, Rafael S. de Souza, Alain Coc, and Christian Iliadis, “Bayesian estimation of the $\text{D}(p,\gamma){}^3\text{He}$ thermonuclear reaction rate,” *The Astrophysical Journal* **923**, 49 (2021).
- [28] P. A. R. Ade *et al.*, “Planck2015 results: XIII. cosmological parameters,” *Astronomy & Astrophysics* **594**, A13 (2016).
- [29] Cyril Pitrou, Alain Coc, Jean-Philippe Uzan, and Elisabeth Vangioni, “A new tension in the cosmological model from primordial deuterium?” *Monthly Notices of the Royal Astronomical Society* **502**, 2474–2481 (2021).
- [30] Tsung-Han Yeh, Jessie Shelton, Keith A. Olive, and Brian D. Fields, “Probing physics beyond the Standard Model: limits from BBN and the CMB independently and combined,” *Journal of Cosmology and Astroparticle Physics* **2022**, 046 (2022).
- [31] Julien Lesgourgues, “The Cosmic Linear Anisotropy Solving System (CLASS) I: Overview,” (2011),

- arXiv:1104.2932 [astro-ph.IM].
- [32] Diego Blas, Julien Lesgourgues, and Thomas Tram, “The Cosmic Linear Anisotropy Solving System (CLASS). part II: Approximation schemes,” *Journal of Cosmology and Astroparticle Physics* **2011**, 034–034 (2011).
- [33] Julien Lesgourgues, “The Cosmic Linear Anisotropy Solving System (CLASS) III: Comparison with CAMB for LambdaCDM,” (2011), arXiv:1104.2934 [astro-ph.CO].
- [34] Julien Lesgourgues and Thomas Tram, “The Cosmic Linear Anisotropy Solving System (CLASS) IV: efficient implementation of non-cold relics,” *Journal of Cosmology and Astroparticle Physics* **2011**, 032–032 (2011).
- [35] Antony Lewis, Anthony Challinor, and Anthony Lasenby, “Efficient computation of CMB anisotropies in closed FRW models,” *ApJ* **538**, 473–476 (2000), arXiv:astro-ph/9911177 [astro-ph].
- [36] Cullan Howlett, Antony Lewis, Alex Hall, and Anthony Challinor, “CMB power spectrum parameter degeneracies in the era of precision cosmology,” *J. Cosmology Astropart. Phys.* **1204**, 027 (2012), arXiv:1201.3654 [astro-ph.CO].
- [37] C Giovanetti, M. Lisanti, H Liu, S. Mishra-Sharma, and J. T. Ruderman, “LINX: A Fast, Differentiable, and Extensible Big Bang Nucleosynthesis Package,” (2024) to appear.
- [38] James Bradbury, Roy Frostig, Peter Hawkins, Matthew James Johnson, Chris Leary, Dougal Maclaurin, George Necula, Adam Paszke, Jake VanderPlas, Skye Wanderman-Milne, and Qiao Zhang, “JAX: composable transformations of Python+NumPy programs,” (2018).
- [39] DeepMind, “The DeepMind JAX Ecosystem,” (2020).
- [40] Tsung-Han Yeh, Keith A. Olive, and Brian D. Fields, “The impact of new $d(p, \gamma)^3\text{He}$ rates on Big Bang Nucleosynthesis,” *JCAP* **03**, 046 (2021), arXiv:2011.13874 [astro-ph.CO].
- [41] Brian D. Fields, Keith A. Olive, Tsung-Han Yeh, and Charles Young, “Big-Bang Nucleosynthesis after Planck,” *JCAP* **03**, 010 (2020), [Erratum: *JCAP* **11**, E02 (2020)], arXiv:1912.01132 [astro-ph.CO].
- [42] Y. Xu, K. Takahashi, S. Goriely, M. Arnould, M. Ohta, and H. Utsunomiya, “NACRE II: an update of the nacre compilation of charged-particle-induced thermonuclear reaction rates for nuclei with mass number $A < 16$,” *Nuclear Physics A* **918**, 61–169 (2013).
- [43] Cyril Pitrou, Alain Coc, Jean-Philippe Uzan, and Elisabeth Vangioni, “Resolving conclusions about the early Universe requires accurate nuclear measurements,” *Nature Rev. Phys.* **3**, 231–232 (2021), arXiv:2104.11148 [astro-ph.CO].
- [44] Joshua S. Speagle, “DYNESTY: a dynamic nested sampling package for estimating Bayesian posteriors and evidences,” *MNRAS* **493**, 3132–3158 (2020), arXiv:1904.02180 [astro-ph.IM].
- [45] Sergey Kopusov, Josh Speagle, Kyle Barbary, Gregory Ashton, Ed Bennett, Johannes Buchner, Carl Scheffler, Ben Cook, Colm Talbot, James Guillochon, Patricio Cubillos, Andrés Asensio Ramos, Ben Johnson, Dustin Lang, Ilya, Matthieu Dartiailh, Alex Nitz, Andrew McCluskey, and Anne Archibald, “dynesty: v2.1.3,” (2023), version 2.1.3. License type: other-open.
- [46] John Skilling, “Nested Sampling,” in *Bayesian Inference and Maximum Entropy Methods in Science and Engineering: 24th International Workshop on Bayesian Inference and Maximum Entropy Methods in Science and Engineering*, American Institute of Physics Conference Series, Vol. 735, edited by Rainer Fischer, Roland Preuss, and Udo Von Toussaint (AIP, 2004) pp. 395–405.
- [47] John Skilling, “Nested sampling for general Bayesian computation,” *Bayesian Analysis* **1**, 833 – 859 (2006).
- [48] F. Feroz, M. P. Hobson, and M. Bridges, “MULTINEST: an efficient and robust Bayesian inference tool for cosmology and particle physics,” *MNRAS* **398**, 1601–1614 (2009), arXiv:0809.3437 [astro-ph].
- [49] Radford M. Neal, “Slice sampling,” *The Annals of Statistics* **31**, 705 – 767 (2003).
- [50] W. J. Handley, M. P. Hobson, and A. N. Lasenby, “polychord: nested sampling for cosmology,” *MNRAS* **450**, L61–L65 (2015), arXiv:1502.01856 [astro-ph.CO].
- [51] W. J. Handley, M. P. Hobson, and A. N. Lasenby, “POLYCHORD: next-generation nested sampling,” *MNRAS* **453**, 4384–4398 (2015), arXiv:1506.00171 [astro-ph.IM].
- [52] Greg Ashton, Noam Bernstein, Johannes Buchner, Xi Chen, Gábor Csányi, Andrew Fowlie, Farhan Feroz, Matthew Griffiths, Will Handley, Michael Habeck, Edward Higson, Michael Hobson, Anthony Lasenby, David Parkinson, Livia B. Pártay, Matthew Pitkin, Doris Schneider, Joshua S. Speagle, Leah South, John Veitch, Philipp Wacker, David J. Wales, and David Yallup, “Nested sampling for physical scientists,” *Nature Reviews Methods Primers* **2** (2022), 10.1038/s43586-022-00121-x.
- [53] P. A. Zyla *et al.*, “The review of particle physics (2020),” *Progress of Theoretical and Experimental Physics* **2020**, 083C01 (2020), pDG 2020.
- [54] Nils Schöneberg, “The 2024 BBN baryon abundance update,” (2024), arXiv:2401.15054 [astro-ph.CO].
- [55] N. Aghanim *et al.*, “Planck2018 results: V. CMB power spectra and likelihoods,” *Astronomy & Astrophysics* **641**, A5 (2020).
- [56] P. A. R. Ade *et al.*, “Planck2013 results. XVI. cosmological parameters,” *Astronomy & Astrophysics* **571**, A16 (2014).
- [57] Antony Lewis and Sarah Bridle, “Cosmological parameters from CMB and other data: A Monte Carlo approach,” *Phys. Rev. D* **66**, 103511 (2002), arXiv:astro-ph/0205436 [astro-ph].
- [58] Thejs Brinckmann and Julien Lesgourgues, “Montepython 3: boosted mcmc sampler and other features,” (2018), arXiv:1804.07261 [astro-ph.CO].
- [59] Nashwan Sabti, James Alvey, Miguel Escudero, Malcolm Fairbairn, and Diego Blas, “Refined Bounds on MeV-scale Thermal Dark Sectors from BBN and the CMB,” *JCAP* **01**, 004 (2020), arXiv:1910.01649 [hep-ph].
- [60] Nashwan Sabti, James Alvey, Miguel Escudero, Malcolm Fairbairn, and Diego Blas, “Addendum: Refined bounds on MeV-scale thermal dark sectors from BBN and the CMB,” *JCAP* **08**, A01 (2021), arXiv:2107.11232 [hep-ph].
- [61] Cara Giovanetti, Mariangela Lisanti, Hongwan Liu, and Joshua T. Ruderman, “Joint Cosmic Microwave Background and Big Bang Nucleosynthesis Constraints on Light Dark Sectors with Dark Radiation,” *Phys. Rev. Lett.* **129**, 021302 (2022), arXiv:2109.03246 [hep-ph].

- [62] Rui An, Vera Gluscevic, Erminia Calabrese, and J. Colin Hill, “What does cosmology tell us about the mass of thermal-relic dark matter?” *JCAP* **07**, 002 (2022), [arXiv:2202.03515 \[astro-ph.CO\]](#).
- [63] Asher Berlin and Nikita Blinov, “Thermal Dark Matter Below an MeV,” *Phys. Rev. Lett.* **120**, 021801 (2018), [arXiv:1706.07046 \[hep-ph\]](#).
- [64] Cara Giovanetti, Martin Schmaltz, and Neal Weiner, “Neutrino-Dark Sector Equilibration and Primordial Element Abundances,” (2024), [arXiv:2402.10264 \[hep-ph\]](#).
- [65] Paul Frederik Depta, Marco Hufnagel, and Kai Schmidt-Hoberg, “Updated BBN constraints on electromagnetic decays of MeV-scale particles,” *JCAP* **04**, 011 (2021), [arXiv:2011.06519 \[hep-ph\]](#).
- [66] Peter Adshead, Pranjal Ralegankar, and Jessie Shelton, “Dark radiation constraints on portal interactions with hidden sectors,” *JCAP* **09**, 056 (2022), [arXiv:2206.13530 \[hep-ph\]](#).
- [67] Nils Schöneberg, Julien Lesgourgues, and Deanna C. Hooper, “The BAO+BBN take on the Hubble tension,” *JCAP* **10**, 029 (2019), [arXiv:1907.11594 \[astro-ph.CO\]](#).
- [68] Daniel Foreman-Mackey, “corner.py: Scatterplot matrices in python,” *The Journal of Open Source Software* **1**, 24 (2016).
- [69] Patrick Kidger, *On Neural Differential Equations*, Ph.D. thesis, University of Oxford (2021).
- [70] Patrick Kidger and Cristian Garcia, “Equinox: neural networks in JAX via callable PyTrees and filtered transformations,” Differentiable Programming workshop at Neural Information Processing Systems 2021 (2021).
- [71] J. D. Hunter, “Matplotlib: A 2D graphics environment,” *Computing in Science & Engineering* **9**, 90–95 (2007).
- [72] Charles R. Harris *et al.*, “Array programming with NumPy,” *Nature* **585**, 357–362 (2020).
- [73] Adrian M. Price-Whelan and Daniel Foreman-Mackey, “schwimmbad: A uniform interface to parallel processing pools in python,” *The Journal of Open Source Software* **2** (2017), [10.21105/joss.00357](#).
- [74] SciPy 1.0 Contributors, “SciPy 1.0: Fundamental Algorithms for Scientific Computing in Python,” *Nature Methods* **17**, 261–272 (2020).

Appendix A: Computational Analysis Details

We use nested sampling [46, 47], as implemented by dynesty [44, 45], with a static sampling method [48–51]. In the analyses reported in this paper and in Appendix B, we sample using 1000 (500) live points for BBN-only (CMB+BBN) analyses and stop when the change in the log of the remaining evidence is 0.5.

The BBN-only analyses take place on 36 Lenovo SD650 standard-memory cores. Including marginalization, these scans take roughly 3-6 CPU-hours to complete (5-10 minutes wall-clock time). The joint analyses are more resource-intensive due to CLASS’s runtime, running on 192 Lenovo SD650 standard-memory cores in $\sim 8,500$ CPU-hours (~ 2 days wall-clock time).

Appendix B: Tabulated Results

Table B1 compiles the results of all analyses performed in this work. The first block includes results from BBN-only analyses without any marginalization of BBN nuisance parameters. These are only intended to be compared with results from marginalizing nuisance parameters in the next block, as well as for comparison with existing results in the literature. *Parameters in this block should not be taken as results or used in future work*—only the results that include marginalization over the nuclear rates should be used.

Similarly, we include results from CMB-only analyses (with Planck nuisance parameters marginalized over) for easy comparison with the results from the CMB+BBN joint analyses (with both Planck and BBN nuisance parameters marginalized over) in the last two blocks. We also show results from other studies in the literature when they can be directly compared with LINX results. These come from Ref. [54] for BBN-only results and Ref. [1] for CMB-only results. In all cases where a comparison is possible, the results from our analyses are in excellent agreement with existing results.

Appendix C: Variation of Uncertainty

In the text, we remark that previous analyses, such as those that appear in Ref. [1] and the PARthENoPE analysis in Ref. [54], assume a constant theory uncertainty on D/H . In general, however, the uncertainty on this prediction varies as a function of N_{eff} and $\Omega_b h^2$. Fig. C1 depicts the uncertainty on D/H in the PRIMAT network, calculated using LINX. This data is obtained by sampling 200 different sets of values for the nuisance parameters at each point on the grid and then finding the standard deviation $\sigma_{D/H}$ of the resulting D/H at each parameter point. $\sigma_{D/H}$ is not constant in the range of interest for N_{eff} and $\Omega_b h^2$ in the $\Omega_b h^2 + N_{\text{eff}}$ model. Instead, $\sigma_{D/H}$ fluctuates by $\sim 30\%$ throughout this range; this is in contrast to, for example, the adoption of a constant $\sigma_{D/H} \simeq 0.03$ in Ref. [1]. When we perform our analyses using LINX, including both model and nuisance parameters, there is a reduction in the error bars compared to previous work that assumes a constant theory uncertainty, as noted in Fig. 1 in the main text.

The variation in $\sigma_{D/H}$ is unknown for any model other than $\Lambda\text{CDM} + N_{\text{eff}}$, either as a function of these parameters or as a function of parameters in a new-physics model. Since the only way to obtain a reliable estimate for $\sigma_{D/H}$ is to perform the sampling described above in the first place, there is no practical reason not to perform a proper marginalization over BBN nuisance parameters using LINX, *e.g.* within the context of an MCMC sampler.

BBN Rates	ν_{BBN} Marginalization	Planck	$100\Omega_b h^2$	$100\Omega_b h^2$ Reference	N_{eff}	N_{eff} Reference	Reference
BBN only, no marginalization over nuclear rates							
PRIMAT	✘	✘	$2.192^{+0.016}_{-0.016}$	–	✘	✘	–
PRIMAT	✘	✘	$2.173^{+0.051}_{-0.050}$	–	$2.94^{+0.28}_{-0.27}$	–	–
YOF	✘	✘	$2.232^{+0.017}_{-0.016}$	$2.234^{+0.016}_{-0.016}$	✘	✘	[54]
YOF	✘	✘	$2.209^{+0.056}_{-0.050}$	–	$2.91^{+0.32}_{-0.26}$	–	–
PARthENoPE	✘	✘	$2.229^{+0.016}_{-0.015}$	–	✘	✘	–
PARthENoPE	✘	✘	$2.209^{+0.054}_{-0.052}$	–	$2.93^{+0.29}_{-0.28}$	–	–
BBN only, marginalized over nuclear rates							
PRIMAT	✔	✘	$2.191^{+0.022}_{-0.021}$	$2.195^{+0.021}_{-0.021}$	✘	✘	[54]
PRIMAT	✔	✘	$2.171^{+0.056}_{-0.051}$	$2.172^{+0.055}_{-0.055}$	$2.93^{+0.30}_{-0.27}$	$2.92^{+0.28}_{-0.28}$	[54]
YOF	✔	✘	$2.233^{+0.060}_{-0.056}$	$2.231^{+0.055}_{-0.055}$	✘	✘	[54]
YOF	✔	✘	$2.214^{+0.079}_{-0.073}$	$2.212^{+0.072}_{-0.072}$	$2.96^{+0.28}_{-0.30}$	$2.93^{+0.27}_{-0.27}$	[54]
PARthENoPE	✔	✘	$2.228^{+0.024}_{-0.023}$	–	✘	✘	–
PARthENoPE	✔	✘	$2.209^{+0.053}_{-0.053}$	–	$2.93^{+0.28}_{-0.28}$	–	–
CMB only, marginalized over Planck nuisance parameters							
✘	✘	✔	$2.231^{+0.015}_{-0.014}$	$2.236^{+0.015}_{-0.015}$	✘	✘	[1]
✘	✘	✔	$2.223^{+0.021}_{-0.021}$	$2.224^{+0.022}_{-0.022}$	$2.95^{+0.19}_{-0.18}$	$2.92^{+0.19}_{-0.19}$	[1]
CMB+BBN, marginalized over both nuclear rates and Planck nuisance parameters							
PRIMAT	✔	✔	$2.218^{+0.012}_{-0.011}$	–	✘	✘	–
PRIMAT	✔	✔	$2.223^{+0.018}_{-0.018}$	–	$3.08^{+0.13}_{-0.13}$	–	–
YOF	✔	✔	$2.233^{+0.014}_{-0.014}$	–	✘	✘	–
YOF	✔	✔	$2.225^{+0.021}_{-0.020}$	–	$2.94^{+0.16}_{-0.16}$	–	–
PARthENoPE	✔	✔	$2.232^{+0.012}_{-0.012}$	–	✘	✘	–
PARthENoPE	✔	✔	$2.225^{+0.020}_{-0.019}$	–	$2.98^{+0.14}_{-0.13}$	–	–

TABLE B1. Median inferred parameters and 68% credible intervals for: 1) BBN-only with no marginalization over BBN nuisance parameters, 2) BBN-only with marginalization over nuisance parameters, 3) CMB-only with marginalization over Planck nuisance parameters, and 4) BBN+CMB joint analyses with marginalization over both Planck and BBN nuisance parameters. The symbol ✘ indicates that a given item is not included in the analysis, while the symbol ✔ indicates that item is included in the analysis. ‘–’ indicates that a reference does not exist—references are provided only where equivalent analyses have been performed, rather than simplified analyses. We use D/H from Ref. [6] and Y_{P} from Ref. [8] as measured values for the BBN likelihood and also in the reference results. Parameters from Ref. [1] are taken for TTTEEE+lowT+lowE.

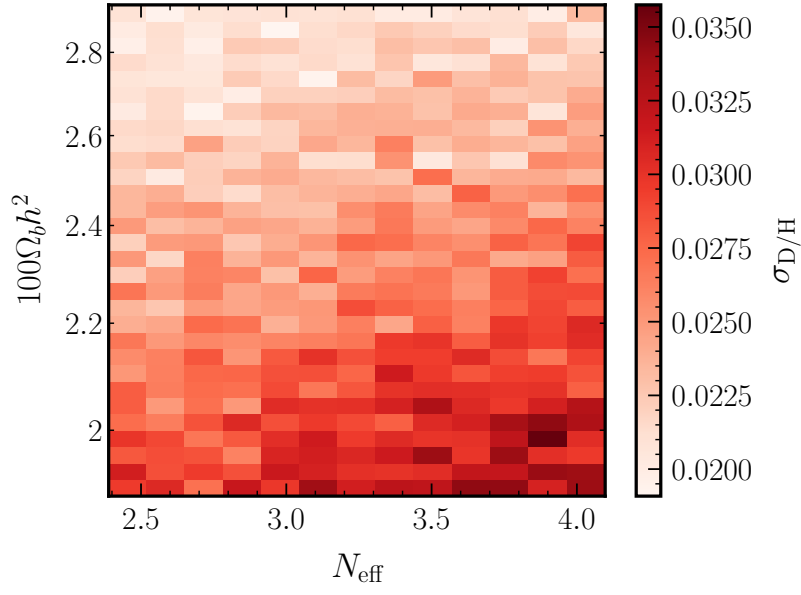


FIG. C1. Variation in the standard deviation for the prediction of D/H in the PRIMAT network as a function of model parameters N_{eff} and $\Omega_b h^2$, obtained by sampling 200 different sets of values for the BBN nuisance parameters at each point in the grid.